Clays and Clay Minerals, Vol. 54, No. 2, 220–229, 2006.

EFFECT OF ACID TREATMENT AND ALKALI TREATMENT ON NANOPORE PROPERTIES OF SELECTED MINERALS

GRZEGORZ JOZEFACIUK* AND DOROTA MATYKA-SARZYNSKA

Institute of Agrophysics of Polish Academy of Sciences, Doswiadczalna 4 str., 20-290 Lublin, Poland

Abstract—Bentonite, biotite, illite, kaolin, muscovite, vermiculite and zeolite were acidified or alkalized with HCl or NaOH of concentrations 0.0, 0.1, 1.0 and 5.0 mole dm^{-3} at room temperature for 2 weeks and converted into Ca homoionic forms. Low-temperature nitrogen and room-temperature water-vapor adsorption-desorption isotherms were used to characterize the mineral pores of radii between 1 and 30 nm. Nanopore volumes, size distributions, average radii and fractal dimensions were calculated. Values calculated from the nitrogen isotherms differed from those derived from water-vapor data. With an increase of the acid-treatment concentration, the pore volumes measured using both adsorption techniques increased markedly for all minerals. The pore radii measured from nitrogen isotherms appeared to decrease for all minerals except zeolite, while the pore radius calculated from water-vapor data increased in most cases. The fractal dimension measured from water vapor isotherms decreased in all cases indicating smoothing of the mineral surfaces and decrease in pore complexity. No well defined trends in any of the pore parameters listed above were noted under alkaline treatment. In the reaction of each mineral with acid and alkali treatments, the individual character of the mineral and the presence of impurities seems important.

Key Words—Acidification, Alkalization, Desorption Isotherms, Fractal Dimension, Minerals, Nanopores.

INTRODUCTION

Many natural bodies, including minerals, are highly porous as a result of their complex structure and the granular character of the solid phase. The basic characteristic of such bodies is provided by a pore-size distribution function showing fractions of pores of different radii while the overall amount of the pores is characterized by the pore volume or bulk density of the material (Rouquerol *et al.*, 1994). The pore system of many porous bodies is geometrically similar under different magnifications which can be characterized by a fractal dimension (Mandelbrot, 1982). The fractal dimension is a measure of the complexity of the porous system and if it is fractal, the greater fractal dimension characterizes the more complex one. As a rule, the fractal behavior of a pore system occurs in a limited range of pore dimensions, called upper and lower cutoffs (Pachepsky *et al.*, 1995). The adsorption-desorption isotherm is an efficient tool for characterizing porous materials in a nanopore range, *i.e.* to estimate pore amount (volume), size distribution (Hernandez *et al.*, 2000) and fractal scaling (El Shafei *et al.*, 2004; Neimark, 1990, 1992).

A pore system of natural bodies results not only from their genesis but also from various environmental factors, among which pH is of primary importance. Acid and alkali effects control mineral weathering and genesis (Yatsu, 1988). Recent increases in soil acidification caused by atmospheric deposition and improper soil nutrition as well as by an increase in the area of alkali- and salt-affected soils have meant that a proper understanding of the mechanisms and parameters controlling soil response to pH changes has become very important (Ulrich, 1990; Tanji, 1995). To understand these processes better, the pH-dependent behavior of soil constituents, *i.e.* soil minerals, among others, should be known. For industrial and environmental protection reasons, there is increasing interest in treatment of minerals with inorganic acids of rather high concentrations and usually at elevated temperatures, referred to as 'acid activation' to produce specific sorbents or catalysts (white carbon blacks). In all the above-mentioned processes, a fine pore system of the minerals is modified, which leads to changes in catalytic, sorption and environmental functions of the minerals. Alteration of fine pores is due at first to changes in the crystal structure of the minerals via dissolution of structural ions and/or rearrangement of the structure under acid or alkali attack. Similar dissolution pathways are observed for various minerals under acid treatment involving structure destruction and formation of silicon oxides (Madejová *et al.*, 1988; Breen and Watson, 1998; Komadel *et al.*, 1990; Šuchá *et al.*, 2001; Kooyman *et al.*, 1997). Alkaline environments affect the composition and the structure of minerals to a lesser extent than an acidic environment (Eberl *et al.*, 1993; Rassineux *et al.*, 2001). However, the formation of new phases, mostly zeolites, occurs frequently under alkaline conditions (Bauer and Velde, 1999; Chermak and Rimstidt, 1987;

* E-mail address of corresponding author:
jozefaci@demeter.ipan.lublin.pl
DOI: 10.1346/CCMN.2006.0540207

Copyright © 2006, The Clay Minerals Society

https://doi.org/10.1346/CCMN.2006.0540207 Published online by Cambridge University Press

de la Villa *et al.*, 2001; Huang, 1993; Taubald *et al.*, 2000).

Generally, more is known about pore behavior of minerals under acid than under alkali treatment. Dekany *et al.* (1999) found that with an increase in the amount of Fe and Al extracted from a sepiolite, the originally microporous structure is transformed to a mesoporous one. They observed a decrease in the surface fractal dimension (from 2.35 to 2.03) after the clay structure was transformed into X-ray amorphous silica-alumina. Balcı (1999) found that the micropore volume increased by up to 20% for the acid-treated sepiolite. Myriam *et al.* (1998) attributed an increase in the specific surface area of a sepiolite and palygorskite after boiling HCl treatment to cleaning and disaggregation of the particles and increasing the number of micropores. Srasra and Trabelsi-Ayedi (2000) reported an increase in porosity and microporosity of a glauconite related to treatment time with boiling HCl. Notario *et al.* (1995) observed an increase in pore volume of natural phillipsite with increasing concentrations of orthophosphoric acid, and this behavior was more pronounced at the microporosity level (<2 nm). Temuujin *et al.* (2004) observed the formation of 3–10 nm pores, in the porous silica product of acid-leached montmorillonite. Hernandez *et al.* (2000) found that acid-treated clinoptilolite reveals a large number of micropores that produced a low-pressure adsorption-desorption hysteresis loop. However, Suarez Barrios *et al.* (1995) reported no creation of microporosity during the HCl treatment of a palygorskite. Molinard *et al.* (1994) treated alumina-pillared montmorillonite with NaOH finding a small decrease in micropore volume and interlayer distance while the acid modification showed an increase in micropore volume.

Jozefaciuk and Bowanko (2002) and Jozefaciuk (2002) studied the effect of acid and alkaline treatment on dissolution patterns and mineralogical, surface and charge properties of bentonite, biotite, illite, kaolin, vermiculite and zeolite. All elements except Si dissolved better in acidic than in alkaline media. However, excluding biotite and vermiculite, the total amount of dissolved solid was greater in 5 N NaOH than in 5 N HCl, due to extreme Si dissolution. In most cases the acid treatment led to severe alteration of the crystal structure of the minerals which was seen from lowering and broadening of the characteristic peaks on the XRD patterns, indicating a decrease in the mineral lattice regularity. An increase in the diffraction intensity at very low angles was attributed to the dispersion and amorphization of the minerals. The XRD patterns and the qualitative composition of dissolved elements for the bentonite indicated that the destruction of the smectite crystallites during acid attack went through interlamellar cation depletion and dissolution of the crystal structure. In the biotite, a new, 14 Å peak appeared, which was practically absent in the untreated mineral, indicating the formation of expanded structures. The intensity of all basal X-ray diffraction (XRD) reflections of the vermiculite decreased sharply under acid attack and the position of the peaks shifted, which indicated that not only the octahedral but also the tetrahedral sheet was severely altered. The presence of mobile octahedral Mg and FeII ions in the vermiculite structure is one reason for its easy destruction on oxides. The zeolite used was not a pure mineral, though significant amorphization of its components was seen from the XRD patterns. Kaolin and illite were most resistant to acid attack.

Much smaller changes in mineral structures were observed in alkaline media. As for the acid treatment, expanded structures were formed in biotite. The alkali treatment frequently led to sharpening of the basal reflections on XRD patterns, explained by the dissolution of the most irregular (X-ray amorphous) parts of the crystal structure ('cleaning' of the minerals). Taking into account the large amount of Si dissolved in alkaline media and the increase in surface acidity, removal of outer silica sheets of the mineral structures thus exposing alumina was also postulated.

Most frequently, water vapor and nitrogen-surface areas, and the variable charge of the minerals increased with an increase in the concentration of acid and alkali treatments, while the adsorption energies and total charge changed in different directions depending on the mineral and the treatment. Weakening of surface acidic character was observed in acidic media.

This work was designed as a continuation of the above-cited studies to gain more knowledge of the complex behavior of minerals in acid and alkaline media. We attempted to look for general patterns of changes in nm-sized pores of the same minerals as used previously and also muscovite under acid and alkali treatments.

MATERIALS AND METHODS

Bentonite (Chmielnik, Poland), biotite (Chongyang, Korea), illite (Yongdong, Korea), kaolin (Vimianzo, Spain), muscovite (Ilmien, Ural Region, Russia), vermiculite (Lovec, Bulgaria) and zeolite (not a pure mineral but with stilbite, natrolite and thomsonite as dominant components, Wolsong, Korea) were studied. The minerals were treated over a 2 week period, at room temperature with hydrochloric acid (H) or sodium hydroxide (OH) solutions of 0.10; 1.0 and 5.0 mole dm^{-3} at a 1:50 solid:liquid ratio. The abbreviated term for each treatment consists of its concentration placed before the H or OH letters (*e.g.* 5OH, see below). The control samples were treated with distilled water. The treatment suspensions were shaken occasionally. After the first week, the treatment solutions were renewed. After the treatments, the solids were washed intensively with 1 mole dm^{-3} of NaCl solution by centrifuging (to avoid eventual precipitation of insoluble

https://doi.org/10.1346/CCMN.2006.0540207 Published online by Cambridge University Press

species that may occur if polyvalent ions are applied). Because adsorption processes on minerals depend strongly on the kind and composition of exchange ions (Cases *et al.*, 1997; Hall and Astill, 1989; Keenan *et al.*, 1951), the samples were converted to Ca homoionic forms by triple 1 mole dm^{-3} $CaCl_2$ treatment followed by washing out of excess salt until there was a negative reaction of the supernatant solution with $AgNO_3$ (isotherms of Ca minerals have more 'classical' shape and are more reproducible; also, washing out Ca chloride excess is much easier than *e.g.* Na chloride due to the lesser 'suspendability' of minerals in solutions containing polyvalent cations). Finally, the samples were air dried and gently powdered in a mortar.

For all treated and control minerals, nitrogen adsorption-desorption isotherms were measured in duplicate at liquid nitrogen temperature using a Sorptomatic 1990 made by Fisons. Taking into account that the differences between two replicates were very small (<0.4%), we decided not to repeat the measurement because of the high costs of the analyses.

Water vapor adsorption-desorption isotherms were measured in triplicate using the vacuum-chamber method at the temperature T = 294±0.1 K. The samples were placed as ~2 mm thick layers in weighing vessels and closed in a vacuum chamber outgassed to ~100 Pa. The relative water-vapor pressure, p/p_0, in the chamber during the adsorption process was controlled by sulfuric acid solutions of stepwise decreasing concentrations (increase of the p/p_0). During the desorption, sulfuric acid solutions of stepwise increasing concentrations were applied. The amount of water present in the samples, a (kg/kg), at a given p/p_0 (calculated from the equilibrium density of H_2SO_4) was measured by weighing after 48 h of equilibration. The dry mass of the samples was estimated after completing adsorption-desorption measurements, after 24 h of oven drying at 378 K. The differences between triplicate measurements of the isotherms did not exceed 2.6% and these were larger for desorption data.

Calculations of pore parameters

The pore radius was calculated from the relative vapor pressure at the desorption using the Kelvin equation. The minimum pore radius was taken as 1 nm corresponding to p/p_0 = 0.342 for water vapor and 0.385 for nitrogen. This meets a frequent assumption that below p/p_0 of ~0.35, surface adsorption processes dominate and the condensation of vapors in pores occurs at higher relative pressures. The maximum pore radius was taken as 30 nm corresponding to p/p_0 = 0.965 for water vapor and 0.969 for nitrogen. In the literature, the maximum pore radius is usually attributed to the highest relative pressure in the experimental window; however, some authors use p/p_0 = 0.96 (Sarikaya *et al.*, 2002) close to the value used in the present work. We selected this value, because the isotherms (particularly the nitrogen ones) become very steep at pressures >0.97−0.98 leading to errors in estimation of pore volumes and sizes.

The pore volume was taken as the volume of the liquid adsorbate retained in a sample during desorption between relative pressure values corresponding to between 30 and 1 nm pore radii. The volume was calculated from the mass and density of the liquid adsorbate.

The average pore radii were evaluated from pore-size distribution functions. These functions were constructed by calculating amounts (fractions) of pores in five ranges of pore radii (equal in logarithmic scale) that provided similar pore-size distribution functions for the replicates of water-vapor desorption data. Despite having more precise data, a similar approach was applied for nitrogen isotherm calculations in order to have a better comparison of the results. The above calculations were performed as described by Jozefaciuk *et al*. (2002).

Fractal dimensions were evaluated from adsorption isotherms. This was performed by fitting the experimentally measured adsorption *vs.* relative pressure data to the linear part of the equation (Neimark, 1990):

$$\ln(a) = C - (1/m)\ln(-\ln(p/p_0)) \quad (1)$$

where C is a constant and the parameter m is related to the surface fractal dimension of the sample. The magnitude of the parameter $1/m$ distinguishes two possible adsorption regimes: when $1/m < 1/3$, the adsorption occurs within the van der Waals regime and the surface fractal dimension is then Ds = $3(1-1/m)$. Alternatively, for $1/m > 1/3$ the adsorption is governed by the capillary condensation mechanism and $D = 3-1/m$. Equation 1 should be applied to the experimental data measured within the multilayer adsorption region, *i.e.* for relatively high relative pressures (Neimark, 1990). Within this region the effects of energetic surface heterogeneity are negligible because the surface-molecule interactions are screened by the particles already adsorbed.

There are doubts amongst previous workers in the area about the ability to relate pore-size distributions and radii (Coasne *et al.*, 2001; Zhu *et al.*, 1998) or fractal dimensions (Crawford and Matsui, 1996) obtained from the isotherms, to particular features of the pore structure, so the pore characteristics calculated in this paper should be treated as comparative parameters for acid- and alkali-treated minerals rather than as absolute values.

RESULTS AND DISCUSSION

Nitrogen adsorption-desorption and water-vapor desorption isotherms for the studied minerals are shown in Figure 1. All nitrogen and most water-adsorption isotherms are of type 2 (S-shaped) BET classification.

Water-vapor isotherms for all biotite samples at low relative pressures ($p/p_0 < 0.4$) resemble a combination of

https://doi.org/10.1346/CCMN.2006.0540207 Published online by Cambridge University Press

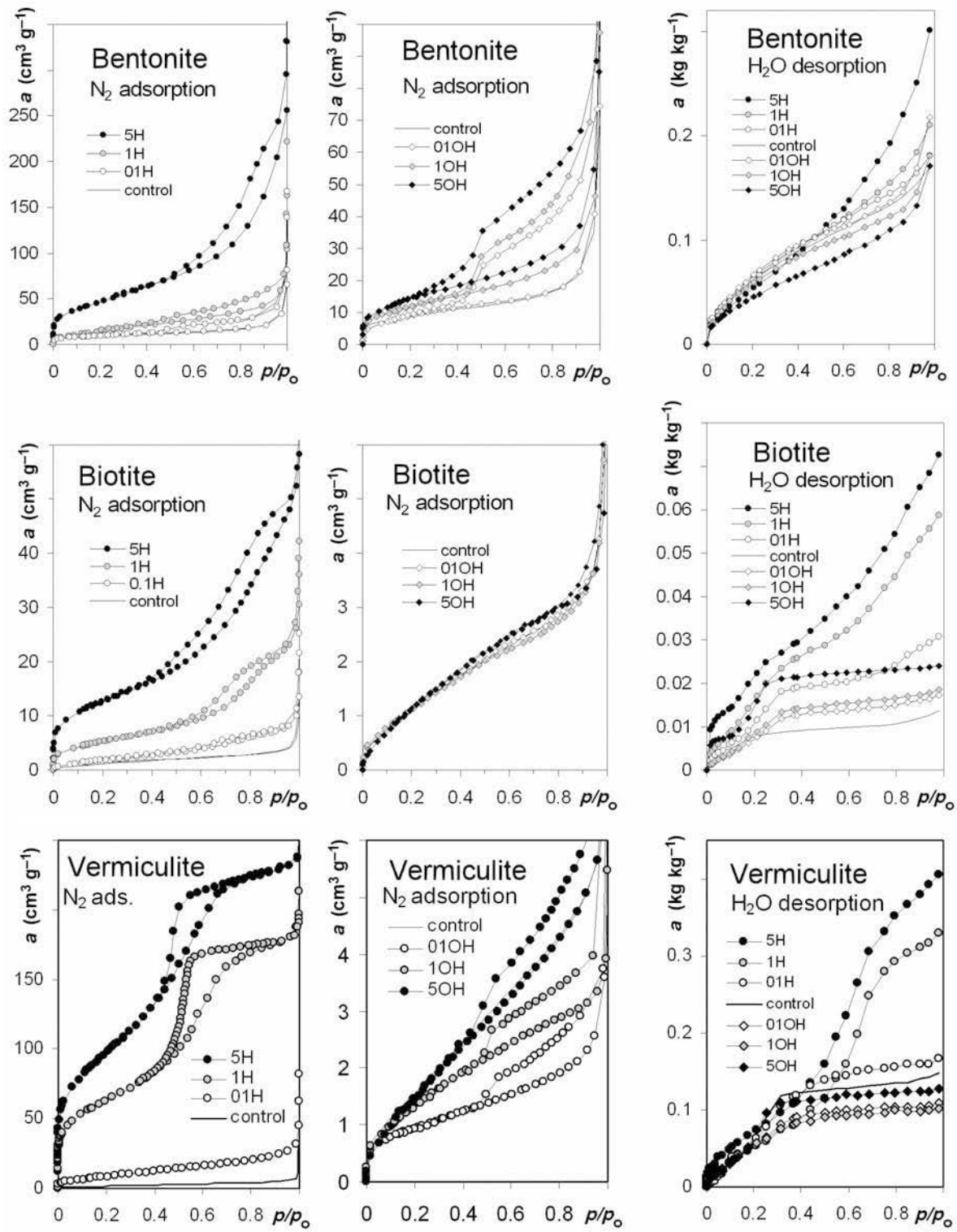

Figure 1. Examples of N_2 adsorption-desorption isotherms and water-vapor desorption isotherms for acid- and alkali-treated minerals. Note that some of the isotherms overlap and are not clearly visible in the graphs (*e.g.* control and 01H biotite).

two Langmuir-type isotherms and the adsorption at medium relative pressures ($0.4 < p/p_0 < 0.8$) seems to be very limited for all samples except 1H and 5H. Similar shapes are shown by vermiculite isotherms, though for these, all but the 1H and 5H samples exhibit limited adsorption also in the high relative pressure range

https://doi.org/10.1346/CCMN.2006.0540207 Published online by Cambridge University Press

(>0.8). Small hysteresis loops are observed in water-vapor adsorption-desorption process for all minerals and treatments so adsorption and desorption isotherms for each sample have very similar shapes.

In nitrogen isotherms, small hysteresis loops are noted for illite, muscovite, kaolinite (both treatments) and for alkali-treated biotite. The hysteresis loops are better developed for zeolite, for which a noticeable decrease in the desorption curve occurs at a p/p_0 value of ~0.5 that corresponds to a pore radius of ~1.4 nm. Well pronounced hysteresis, at ~p/p_0 = 0.5, occurs for all except the control and the 01H vermiculite samples. For the 1H and 5H samples, an almost vertical drop in the desorption curves is noted which may indicate the occurrence of well defined homogeneous pores of cylindrical shape. The desorption isotherms for alkali-treated bentonite show well defined hysteresis loops with a fast decrease in the desorption curves at p/p_0 of ~0.45 (pore radius of ~1.2 nm). Acid-treated bentonite samples show a large hysteresis developed around p/p_0 of 0.8 (pore radius of ~4.3 nm). Similar hysteresis (p/p_0 of ~0.7, R of ~2.7 nm) is shown by acid-treated biotite.

In general, the adsorption of water and nitrogen increases with the increase of both treatment concentration, and the increase in adsorption is usually much higher under acidic than under alkaline treatments. However, a few of the samples treated with low concentrations of acid or alkali adsorb less vapor than the control samples. This is probably due to the dissolution of amorphous phases of high adsorption capacity present in the initial minerals.

Calculated from desorption isotherms, pore-size distribution functions of the untreated minerals are plotted in Figure 2. In general, different distribution functions are calculated from nitrogen and water desorption data for the same mineral (for illite and vermiculite only, both functions are similar). The distribution function for bentonite calculated from water-vapor data shows a prevalence of narrow pores whereas this function calculated from nitrogen isotherms shows that medium and large pores dominate. One may suspect that fine pores in bentonite are more easily available for small and polar water molecules than for the larger and non-polar nitrogen molecules. However, this may be related to the fact that the nitrogen isotherms are usually much steeper than water-vapor isotherms in a high-pressure (large pore) region. For biotite, fractions of pores estimated from water-vapor isotherms are more or less equal in all size ranges studied and nitrogen data show larger numbers of large pores, as for bentonite. Extremely high fractions of large pores show nitrogen pore-size distribution functions for kaolin, while larger fractions of small pores are seen in distribution functions derived from water-vapor data. The latter finding seems surprising, as kaolin particles should not have internal porosity and intergranular porosity (large pores) should dominate, as revealed by nitrogen. The water-vapor pore-distribution functions for illite and muscovite are such as would be expected for non-porous minerals, and have somewhat similar shapes to nitrogen-pore distributions. Both adsorbates detect larger amounts of smaller pores for vermiculite for which an unexpectedly larger number of smaller pores is seen from nitrogen than from water-vapor data; this also holds for zeolite.

The pore volumes, average radii, fractal dimensions and ranges of fractal scaling calculated from the isotherms of the control minerals are shown in Table 1. Water vapor indicates the largest nanopore volumes for bentonite and zeolite and the smallest for biotite and muscovite, whereas the largest pore volumes for bentonite and kaolinite and the lowest for biotite and vermiculite are found from nitrogen data. Differences in pore volumes of the studied minerals are large, reaching a factor of 10, while average pore radii differ by a factor of 2. Water-vapor data show that the largest nanopores are in muscovite, illite and zeolite, and the smallest are in bentonite and vermiculite. Nitrogen isotherms detect the largest nanopores in kaolin and biotite and the smallest nanopores in vermiculite and zeolite. As measured from water-vapor isotherms, the most complex pore system (highest fractal dimension) is in vermiculite, biotite and bentonite, while the least complex pore systems are found in kaolinite and muscovite. This seems logical, knowing the complex crystal structures in the first group of minerals and the lack of internal structures in the second. Surprisingly, nitrogen isotherms show most complicated pore system for kaolinite and illite and the least complex for vermiculite and biotite. In most cases, the fractal dimensions resulting from

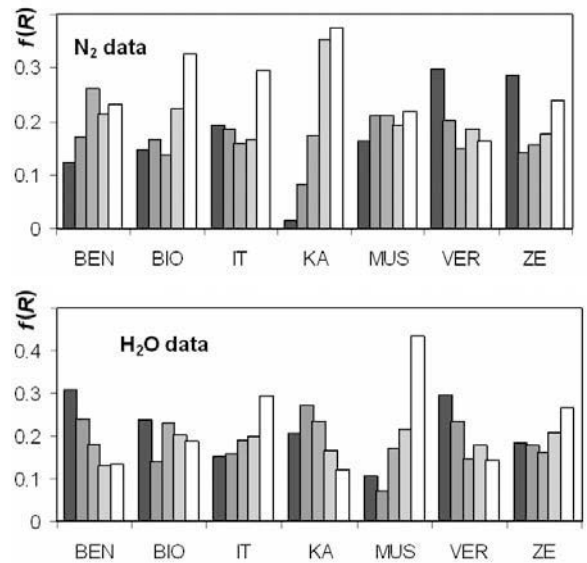

Figure 2. Pore-size distribution functions for the untreated minerals (abbreviated on the horizonal axis). For each mineral, the bars from left to right denote pores of consecutively larger sizes. The five bars correspond to the five pore radii ranges between 1 and 30 nm, equal in logarithmic scale.

https://doi.org/10.1346/CCMN.2006.0540207 Published online by Cambridge University Press

Table 1. Pore parameters for untreated minerals (control samples) measured from water-vapor and nitrogen adsorption-desorption isotherms.

Data	Bentonite	Biotite	Illite	Kaolinite	Muscovite	Vermiculite	Zeolite
V_{H_2O}, mm^3g^{-1}	82.5	4.5	23.4	31	7.2	23.6	67.7
V_{N_2}, mm^3g^{-1}	53.1	4.7	18.7	35.1	17.7	6.6	20.0
R_{H_2O}, nm	6.8	8.7	10.8	7.1	13.6	7.3	10.1
R_{N_2}, nm	9.9	11.4	10.3	13.8	9.2	7.7	9.2
D_{H_2O}	2.83	2.88	2.68	2.34	2.40	2.93	2.70
D_{N_2}	2.66	2.44	2.71	2.82	2.59	2.16	2.62
FR_{H_2O}, p/p_0	0.44–0.93	0.58–0.93	0.21–0.96	0.21–0.81	0.21–0.93	0.34–0.75	0.31–0.94
FR_{N_2}, p/p_0	0.10–0.91	0.26–0.62	0.65–0.98	0.10–0.34	0.45–0.97	0.10–0.5	0.10–0.93

V: pore volume, R: average pore radius, D: fractal dimension, FR: fractality range (V and R are calculated for pores between 1 and 30 nm in radius).

water-vapor adsorption are greater than those estimated from nitrogen-adsorption isotherms. The ranges of fractal scaling for particular minerals are different. However, they overlap more or less for all minerals that can validate the comparison of fractal dimensions. The values of the slopes of the linear parts of the fractal plots for $1/m$ (see equation 1) are >1/3 indicating that adsorption by the studied minerals is governed by the capillary condensation mechanism and this confirms to some extent the applicability of the approach used for pore-parameter calculations. The fractal behavior may also be attributed to surface roughness as far as very small pore dimensions are involved (even <1 nm, which was assumed to be the smallest pore radius).

It is difficult to compare the present data with the literature results because of different pressure ranges used for data reading and calculations. Usually (cited papers), the lowest porosities are reported for kaolinites, moderate values are found for illites, and the largest values for smectites, vermiculites and zeolites. Similar dependencies are observed under natural conditions. For example, Hassan and El-Shall (2004) found that an increase in the relative amounts of kaolin and quartz in three glauconitic minerals containing illite-smectite mixed layers decreased the pore volume. Also, the fractal dimensions calculated from nitrogen adsorption data are least for kaolinite, medium for illite and greatest for montmorillonite (Pernyeszi and Dekany, 2003). Contrary to the present findings, larger fractal dimensions have usually been calculated from nitrogen than from water-vapor data for soils (Sokolowska *et al.*, 1999; Slawinski *et al.*, 2002), and also for cement materials (Niklasson, 1993).

As can be seen, the shapes of adsorption-desorption isotherms, pore-size distribution functions and the calculated pore parameters for each mineral depend on the method used despite the fact that both the water-vapor and nitrogen data come from the same pore-size range. This may be due to different chemical characters of the water and nitrogen molecules (Low, 1961). Also, the nitrogen adsorption method requires prior evacuation and heating of the sample, which makes water films thinner and brings the clay particles closer. The quasi-contact of the mineral plates (for morphological platy clays) can extend over a significant portion of the surfaces; thus the pores between may become inaccessible for non-polar (nitrogen) molecules. If the clay contains expansible interlayers, these collapse on evacuation, giving the same effect. The molecular sieving is believed to differentiate between the entrance of gas molecules of various sizes into narrow spaces (Volzone *et al.*, 1999) leading to differences in porosities. The kinetic effects may diminish the adsorption of nitrogen to a great extent when entrances to larger spaces are of nitrogen molecule dimensions. To easily pass such narrow entrances, the thermal energy of the molecule should be similar to the energy barrier of the adsorption field among the entrance walls. At liquid nitrogen temperature the thermal energy is small and therefore the adsorption equilibrium may not be reached within a standard time of the measurement (Newman, 1985). There are differences in adsorption pathways and so the pore parameters may be due not only to differences in characteristic features of the mineral pore systems, but also to the various extents and intensities of the above-mentioned processes in different minerals.

Changes in pore volumes of the studied minerals under acid and alkali treatments are presented in Figure 3 where the ratio of the pore volume of the treated mineral to the pore volume of the control sample is given. Note that, for better data reading, the points depicting extreme data are shifted against the vertical axis and labeled with their real values. Except for the nitrogen-pore volume for acid- and alkali-treated zeolite and alkali-treated illite, the pore volumes of the studied minerals increase with both acid and alkaline treatments, which is a commonly observed phenomenon. This is in keeping with a sharp increase in specific surface areas and the amount of variably charged surfaces of the minerals under acid and alkali attack, as observed previously (Jozefaciuk and Bowanko, 2002; Jozefaciuk, 2002). A large proportion of the newly formed surfaces may be connected to new pore walls. In a few cases the

https://doi.org/10.1346/CCMN.2006.0540207 Published online by Cambridge University Press

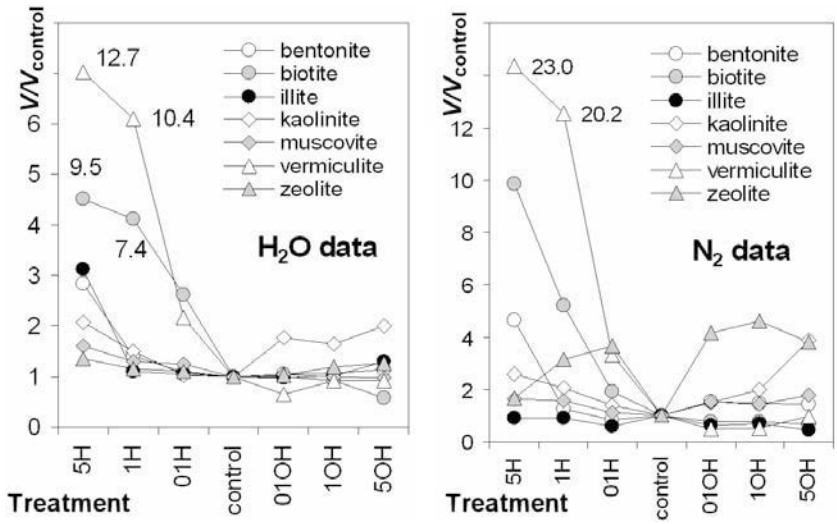

Figure 3. Relative changes in pore volume due to the treatments. On the vertical axis, the ratio of the pore volume of the treated sample to the pore volume of the control sample is given. Some points were shifted towards the vertical axis to have other data more visible. The shifted points are labeled with their real values.

pore volume reduces during treatment at the lowest concentrations; that may be due to 'cleaning' of the minerals of impurities, *e.g.* X-ray amorphous and/or very finely dispersed crystalline solids having large porosities, as mentioned before. Therefore, changes starting from 0.1 N treatments may reflect alterations of minerals better under acid and base attack. The acid treatment affects pore volumes significantly more than the alkaline treatment. The nitrogen pore volumes are more sensitive to the treatments. For example, with treatment in the strongest acid, the nitrogen pore volume of vermiculite increased by a factor of 23, whereas for water, the increase was only half this amount. The greatest increase in the water pore volume after acid treatment occurred for vermiculite and biotite and after alkali treatment for zeolite and kaolinite. The increase in pore volume under acid treatment may be caused by production of finely dispersed Si oxides from destruction and leaching of mineral structures, by removal of X-ray amorphous aluminum or silica components plugging surface pores or interlamellar spaces, by formation of the surface cracks and voids, as well as by decrease in the mineral-particle sizes. Under alkaline conditions, similar processes may occur together with an accumulation of X-ray amorphous Fe and Mg hydroxides (Ca hydroxides were probably dissolved during the washing step).

Changes in average pore radii of the studied minerals under acid and alkali treatments are illustrated in Figure 4 showing ratios of pore radii of treated and control samples. The pore radii calculated from nitrogen isotherms decrease in most cases (zeolite is an exception) under increasing concentration of the acid treat-

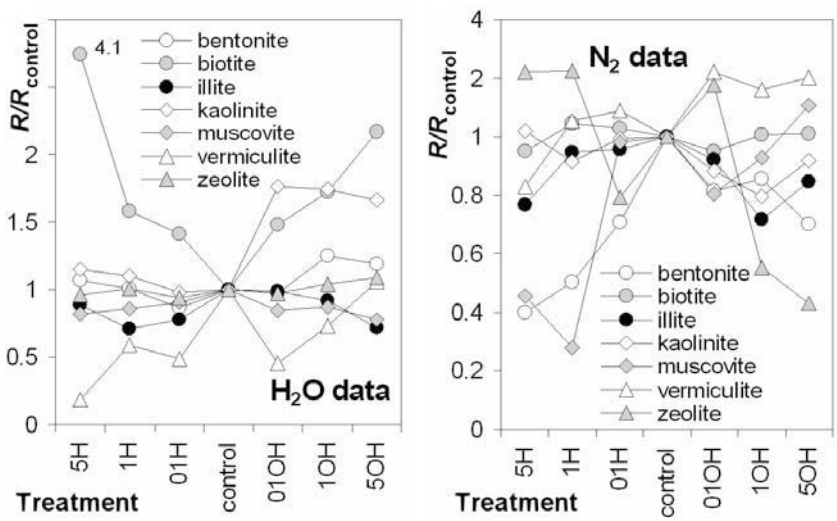

Figure 4. Relative changes in average pore radius due to the treatments. Abbreviations and notes as for Figure 3.

https://doi.org/10.1346/CCMN.2006.0540207 Published online by Cambridge University Press

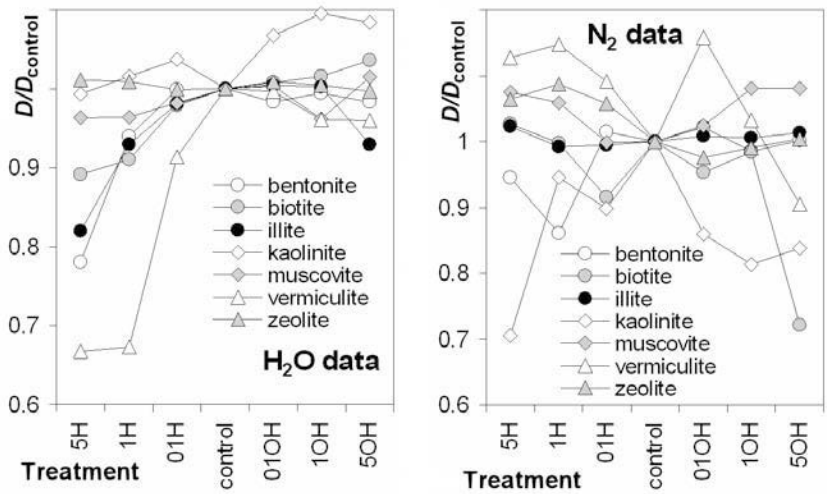

Figure 5. Relative changes in fractal dimension due to the treatments. Abbreviations and notes as for Figure 3.

ment; no definite tendencies are observed under alkali treatment. With the increase of acid-treatment concentration, the average pore radius calculated from water-vapor desorption data increases for biotite, kaolinite and bentonite and decreases for vermiculite and muscovite. Under alkali treatment the water-vapor pore radius increases for biotite, vermiculite and zeolite (slightly) and decreases for illite and kaolinite.

The increase in pore radii may be due to the removal of surface impurities and mineral destruction, and the decrease due to the formation of cracks and voids on the surfaces attacked or in fine pore openings. In many cases the decrease in nitrogen pore radii relates to increasing hysteresis in the isotherms, *i.e.* the sharp decrease in desorption curve at low p/p_0 values that correspond to small pore radii and apparently indicates the formation of small pores. Water desorption isotherms in the low-pressure range are flat. Therefore, the calculated fraction of small pores is large for nitrogen and small for water and most pronounced for acid-treated minerals. The detection of large amounts of small pores by nitrogen and not by water is surprising, as water molecules are smaller in size. This is possibly due to more specific interaction of polar water molecules with polar, hydrophyllic mineral surfaces, suggesting that the adsorption/desorption process has a more polymolecular character in water than in nitrogen. The smaller nitrogen pore radii than comparable water values may also be due to the above phenomenon.

The fractal dimension measured from water-vapor adsorption decreases for all minerals except zeolite (very slight increase) under acid treatment whereas smaller changes in both directions occur under alkali treatment, as presented in Figure 5. A similar decrease in fractal dimension occurs in acidified soils (Jozefaciuk *et al.*, 2002). The nitrogen fractal dimension exhibits no well defined trends under either treatment. The decrease in fractal dimension suggests a decrease in the pore complexity and a smoothing of the surface roughness that can be related to removal of finest mineral particles, X-ray amorphous soil components and surface coatings and dissolution of the most exposed parts of the surfaces. Indeed, one can expect such effects to be due to the acid attack. It is worth noting that X-ray amorphous silica oxides, produced under acid attack, have low water-vapor fractal dimensions also. Various changes in fractal character of the surface can be due to different mechanisms of material dissolution in different minerals or a preferential dissolution of some components. For example, the dissolution of X-ray amorphous material with a high degree of dispersion or cementing agents should lead to the decrease of surface and pore complexity (D decrease) while the partial dissolution of mineral particles and the resulting increase in their degree of dispersion, as well as formation of surface cavities, may lead to an increase in the fractal dimension. The prevailing mechanism has a dominant effect on the fractal behavior. It is important to note that the ranges of fractality usually change under both acid and alkali treatments; however, for each mineral they also overlap.

The changes in porosity characteristics under acid and alkali treatment are summarized in Table 2, showing most of the general trends of the changes observed. In assessing these trends, changes of the given parameter starting from 0.1 N treatment concentrations were frequently taken into account thus ignoring the initial changes, for reasons mentioned previously. One can observe that better pronounced trends in the behavior of a given pore parameter are observed under acid than under alkali treatment. These most general tendencies in the minerals' behavior under acid and alkali treatments may be summarized as follows. Pore volumes measured using both water-vapor and nitrogen isotherms generally increase for all minerals. Pore-radius decrease is

https://doi.org/10.1346/CCMN.2006.0540207 Published online by Cambridge University Press

Table 2. Trends of changes in pore parameters for acid- and alkali-treated minerals measured from water vapor and nitrogen adsorption-desorption isotherms.

Mineral	BE	BI	IL	KA	MU	VE	ZE	BE	BI	IL	KA	MU	VE	ZE
	Acid treatment							Alkali treatment						
V_{H_2O}	I	I	I	I	I	I	I	–	D	–	I	–	I	I
V_{N_2}	I	I	I	I	I	I	D	–	D	D	I	I	I	
R_{H_2O}	I	I	I	I	D	D	–	I	I	D	D	D	I	I
R_{N_2}	D	D	D		D	D	I	D	I			I		D
D_{H_2O}	D	D	D	D	D	D	I		I	D	I		D	D
D_{N_2}		I	D	D	I	I			I		D	I	D	I

Abbreviations: as in Table 1
In the first row, the two letters given are the first two letters of the mineral name.
I: increase; D: increase; –: no significant change; empty cell denotes no defined trend (data scattering).

observed from nitrogen-desorption data, whereas water-vapor data usually show the pore radius increase. The fractal dimension calculated from water-vapor adsorption decreases for all acid-treated minerals. Non-uniform changes in fractal dimension are observed under alkali treatment.

CONCLUSIONS

Except for increases in water-vapor and nitrogen pore volumes and a decrease in water-vapor fractal dimension under acid treatment, no general trends are evident in changes of other nanopore parameters of minerals under acid and/or alkali treatment. Different directions and/or intensities in changes in pore structure for individual minerals even under the same treatment are probably due to the presence and behavior of impurities, as well as to differences in particle size of the minerals, their crystal structure, and surface build up. It seems that an individual explanation should be found for each mineral. This needs more detailed investigation, *e.g.* using scanning microscopy and/or other advanced surface-observation techniques. The data obtained here on changes in nm-sized pores of individual minerals in acidification and alkalization processes may be useful for some industrial, scientific and environmental purposes.

Marked differences in pore parameters obtained by using nitrogen and water-vapor adsorption techniques are noted. Water-vapor isotherms have the advantage that smaller water molecules can detect changes in pore volumes better and certainly in pore-fractal character. The sample pretreatment for water-vapor isotherms measurement also seems to have less effect on the sample than in the case of nitrogen. The nitrogen adsorption/desorption process involves only non-specific interactions between adsorbate and the surface; thus the interpretation of the isotherms in terms of condensation in pores is more evident. The instrumental nitrogen isotherms are also more precise.

REFERENCES

Balcı, S. (1999) Effect of heating and acid pre-treatment on pore size distribution of sepiolite. *Clay Minerals*, **34**, 647–653.

Bauer, A. and Velde, B. (1999) Smectite transformation in high molar KOH solutions. *Clay Minerals*, **34**, 259–273.

Breen, C. and Watson, R. (1998) Acid-activated organoclays: preparation, characterisation and catalytic activity of poly-cation-treated bentonites. *Applied Clay Science*, **12**, 479–494.

Cases, J.M., Berend, I., Francois, M., Uriot, J.P., Michot, L.J. and Thomas, F. (1997) Mechanism of adsorption and desorption of water vapor by homoionic montmorillonite. 3. The Mg, Ca, Sr, and Ba exchanged forms. *Clays and Clay Minerals*, **45**, 8–22.

Chermak, J.A. and Rimstidt, J.D. (1987) The hydrothermal transformation of kaolinite to muscovite/illlite. *Geochimica et Cosmochimica Acta*, **54**, 2979–2990.

Coasne, B., Grosman, A., Dupont-Pavlovsky, N., Ortega, C. and Simon, M. (2001) Adsorption in an ordered and non-interconnected mesoporous material: Single crystal porous silicon. *Physical Chemistry Chemical Physics*, **3**, 1196–1200.

Crawford, J.W. and Matsui, N. (1996) Heterogeneity of the pore and solid volume of soil: distinguishing a fractal space from its non-fractal complement. *Geoderma*, **73**, 183–195.

de la Villa, R.V., Cuevas, J., Ramirez, S. and Leguey, S. (2001) Zeolite formation during the alkaline reaction of bentonite. *European Journal of Mineralogy*, **13**, 635–644.

Dekany, I., Turi, L., Fonseca, A. and Nagy, J.B. (1999) The structure of acid-treated sepiolites: small-angle X-ray scattering and multi MAS-NMR investigations. *Applied Clay Science*, **14**, 141–160.

Eberl, D.D., Velde, B. and McCormick, T. (1993) Synthesis of illite-smectite from smectite at earth surface temperatures and high pH. *Clay Minerals*, **28**, 49–60.

El Shafei, G.M.S., Philip, C.A. and Moussa N.A. (2004) Fractal analysis of hydroxyapatite from nitrogen isotherms. *Journal of Colloid and Interface Science*, **277**, 410–416.

Hall, P.L. and Astill, D.M. (1989) Adsorption of water by homoionic exchange forms of Wyoming bentonite (SWy1). *Clays and Clay Minerals*, **37**, 355–363.

Hassan, M. and El-Shall, H. (2004) Glauconitic clay of El Gidida, Egypt: evaluation and surface modification. *Applied Clay Science*, **27**, 219–222.

Hernandez, M.A., Rojas, F. and Lara, V.B. (2000) Nitrogen-sorption characterization of the microporous structure of clinoptilolite-type zeolites. *Journal of Porous Materials*, **7**, 443–454.

https://doi.org/10.1346/CCMN.2006.0540207 Published online by Cambridge University Press

Huang, W.L. (1993) The formation of illitic clays from kaolinite in KOH solution from 225 to 350ºC. *Clays and Clay Minerals*, **41**, 645–654.

Jozefaciuk, G. (2002) Effect of acid and alkali treatment on surface-charge properties of selected minerals. *Clays and Clay Minerals*, **50**, 646–655.

Jozefaciuk, G. and Bowanko, G. (2002) Effect of acid and alkali treatment on surface areas and adsorption energies of selected minerals. *Clays and Clay Minerals*, **50**, 771–783.

Jozefaciuk, G., Hoffmann, C. and Marschner, B. (2002) Effect of extreme acid and alkali treatment on pore properties of soil samples. *Journal of Plant Nutrition and Soil Science*, **165**, 59–66.

Keenan, A.G., Mooney, R.W. and Wood, L.A. (1951) The relation between exchangeable ions and water adsorption on kaolinite. *Journal of Physical Colloid Chemistry*, **55**, 1462–1474.

Komadel, P., Schmidt, D., Madejová, J. and Čičel, B. (1990) Alteration of smectites by treatments with hydrochloric acid and sodium carbonate solutions. *Applied Clay Science*, **5**, 113–122.

Kooyman, P.J., van der Waal, P. and Van Bekkum, H. (1997) Acid dealumination of ZSM-5. *Zeolites*, **18**, 50–53.

Low, P.F. (1961) Physical chemistry of clay-water interaction. *Advances in Agronomy*, **40**, 269–327.

Madejová, J., Bujdak, J., Janek, M. and Komadel, P. (1998) Comparative FT-IR study of structural modifications during acid treatment of dioctahedral smectites and hectorite. *Spectrochimica Acta A. Molecular and Biomolecular Spectroscopy*, **54**, 1397–1406.

Mandelbrot, B. (1982) *The Fractal Geometry of Nature*. Freeman, San Francisco, USA.

Molinard, A., Clearfield, A., Zhu, H.Y. and Vansant, E.F. (1994) Stability and porosity of alumina-pillared clay in acid and basic solutions. *Microporous Materials*, **3**, 1–2, 109–116.

Myriam, M., Suarez, M. and Martin Pozas, J.M. (1998) Structural and textural modifications of palygorskite and sepiolite under acid treatment. *Clays and Clay Minerals*, **46**, 225–231.

Neimark, A.V. (1990) Calculating fractal dimensions of adsorbents. *Adsorption Science and Technology*, **7**, 210–219.

Neimark, A.V. (1992) A new approach to determination of the surface fractal dimension of porous solids. *Physica Acta*, **191**, 258–262.

Newman, A.C.D. (1985) The interaction of water with clay mineral surfaces. Pp. 237–274 in: *Chemistry of Clays and Clay Minerals* (A.C.D. Newman, editor). Mineralogical Society Monograph **6**. Longman Scientific and Technical, Essex, UK

Niklasson, G.A. (1993) Adsorption on fractal structures application to cement materials. *Cement and Concrete Research*, **23**, 1153–1158

Notario, J.S., Garcia, J.E., Caceres, J.M., Arteaga, I.J. and Gonzalez, M.M. (1995) Characterization of natural phillipsite modified with orthophosphoric acid. *Applied Clay Science*, **10**, 209–217.

Pachepsky, Ya.A., Polubesova, T.A., Hajnos, M., Sokołowska, Z. and Jozefaciuk, G. (1995) Fractal parameters of pore surface area as influenced by simulated soil degradation. *Soil Science Society of America Journal*, **59**, 68–75.

Pernyeszi, T. and Dekany, I. (2003) Surface fractal and structural properties of layered clay minerals monitored by small angle X-ray scattering and low-temperature nitrogen adsorption experiments. *Colloid Polymer Science,* **281**, 73–78.

Rassineux, F., Griffault, L., Meunier, A., Berger, G., Petit, S., Vieillard, P., Zellagui, R. and Munoz, M. (2001) Expandability-layer stacking relationship during experimental alteration of a Wyoming bentonite in pH 13.5 solutions at 35 and 60ºC. *Clay Minerals*, **36**, 197–210.

Rouquerol, R., Avnir, D., Fairbridge, C.W., Everett, D.H., Haynes, J.H., Pernicone, N., Ramsay, J.D.F., Sing, K.S.W. and Unger, K.K. (1994) Recommendations for the characterization of porous solids. *Pure Applied Chemistry* **66**, 1739–1758.

Sarikaya, Y., Alemdaroglu, T. and Onal, M. (2002) Determination of the shape, size and porosity of fine α-Al_2O_3 powders prepared by emulsion evaporation. *Journal of the European Ceramic Society*, **22**, 305–309.

Slawinski, C., Sokolowska, Z., Walczak, R., Borowko, R. and Sokolowski, S. (2002) Fractal dimension of peat soils from adsorption and from water retention experiments. *Colloids and Surfaces A. Physicochemical and Engineering Aspects*, **208**, 289–301.

Sokolowska, Z., Hajnos, M., Borowko, M. and Sokołowski, S. (1999) Adsorption of nitrogen on thermally treated peat soils. The role of energetic and geometric heterogeneity. *Journal of Colloid and Interface Science* **219**, 1–10.

Srasra, E. and Trabelsi-Ayedi, M. (2000) Textural properties of acid activated glauconite. *Applied Clay Science*, **17**, 71–84.

Suarez Barrios, M., Flores González, L.V., Vicente Rodríguez, M.A. and Martín Pozas, J.M. (1995) Acid activation of a palygorskite with HCl: Development of physico-chemical, textural and surface properties. *Applied Clay Science*, **10**, 247–258.

Šuchá, V., Środoń, J., Clauer, N., Elsass, F., Eberl, D.D., Kraus, I. and Madejová, J. (2001) Weathering of smectite and illite-smectite under temperate climatic conditions. *Clay Minerals*, **36**, 403–419.

Tanji, K.N. (1995) *Agricultural Salinity Assessment and Management*. Scientific Publishers, Jodphur, India.

Taubald, H., Bauer, A., Schafer, T., Geckeis, H. and Satir, M. (2000) Experimental investigation of the effect of high-pH solutions on the Opalinus Shale and the Hammerschmiede Smectite. *Clay Minerals*, **35**, 515–524.

Temuujin, J., Jadamba, T., Burma, G., Erdenechimeg, S., Amarsana, J. and MacKenzie, K.J.D. (2004) Characterisation of acid activated montmorillonite clay from Tuulant (Mongolia). *Ceramics International*, **30**, 251–255

Ulrich, B. (1990) *An Ecosystem Approach to Soil Acidification*. Pp. 28–79 in: *Soil Acidity* (B. Ulrich and M.E. Sumner, editors). Springer-Verlag, Berlin.

Volzone, C., Thompson, J.G., Melnitchenko, A., Ortiga, J. and Palethorpe, S.R. (1999) Selective gas adsorption by amorphous clay-mineral derivatives. *Clays and Clay Minerals*, **5**, 647–657.

Yatsu, E. (1988) *The Nature of Weathering. An Introduction*. Sozosha, Tokyo.

Zhu, H.Y., Lu, G.Q. and Zhao, X.S. (1998) Thickness and stability of adsorbed film in cylindrical mesopores. *Journal of Physical Chemistry,* **102**, 7371–7376.

(*Received 8 June 2005; revised 28 November 2005; Ms. 1060; A.E. Peter Komadel*)

https://doi.org/10.1346/CCMN.2006.0540207 Published online by Cambridge University Press